Electronic Supplementary Information

Synthesis and Characterization of $(Ga_{1-x}Zn_x)(N_{1-x}O_x)$ Nanocrystals with a Wide Range of Compositions

Kyureon Lee,[†] Ying-Gang Lu,[†] Chi-Hung Chuang,[†] Jim Ciston,[#] Gordana Dukovic[†]*

[†]Department of Chemistry and Biochemistry, University of Colorado Boulder, Boulder, Colorado 80309, United States

[#]National Center for Electron Microscopy, Molecular Foundry, Lawrence Berkeley National Laboratory, Berkeley, California 94720, United States

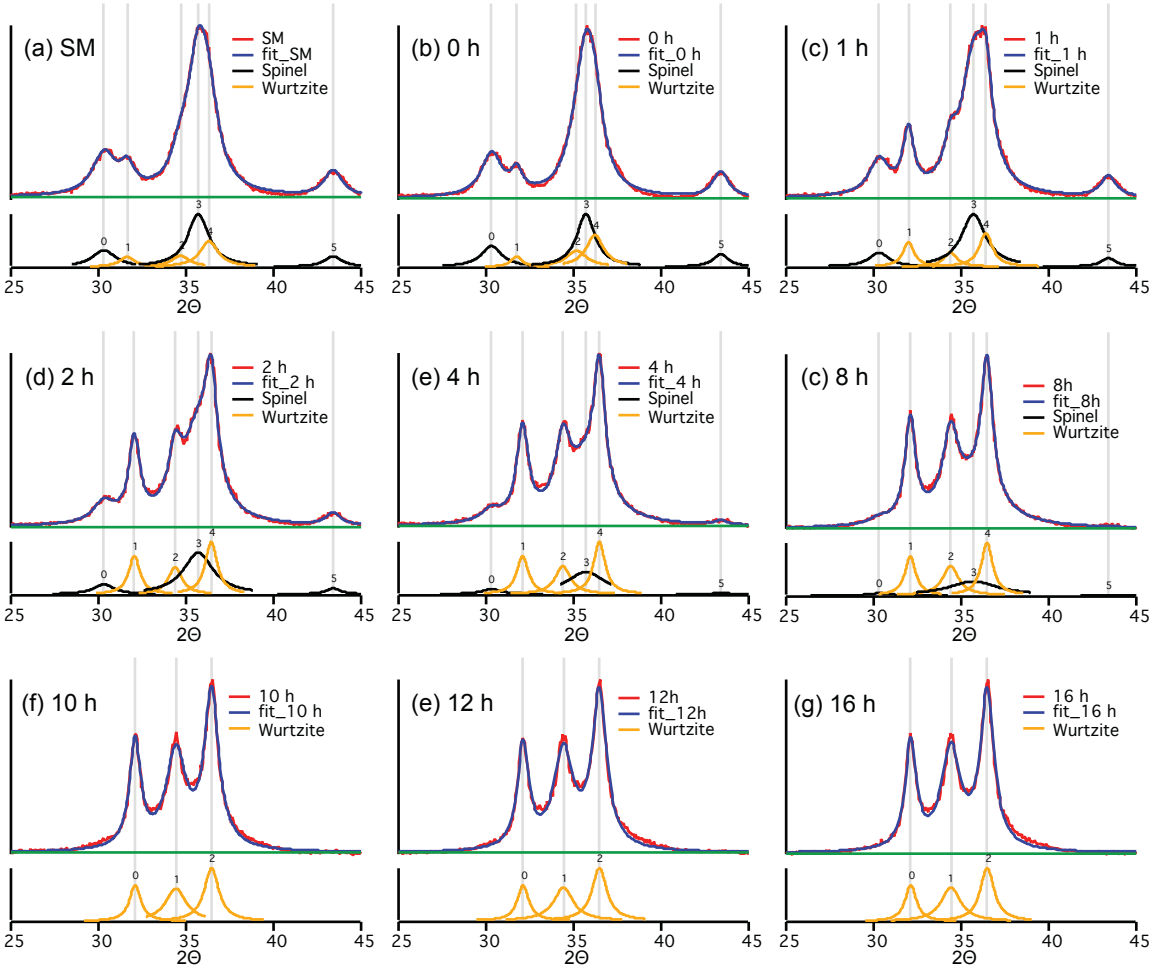

Figure S1. Fitting of XRD patterns of the nitrided products for 0–16 hours at 650 °C from a starting material mixture with Zn/(Zn+Ga)=0.39.

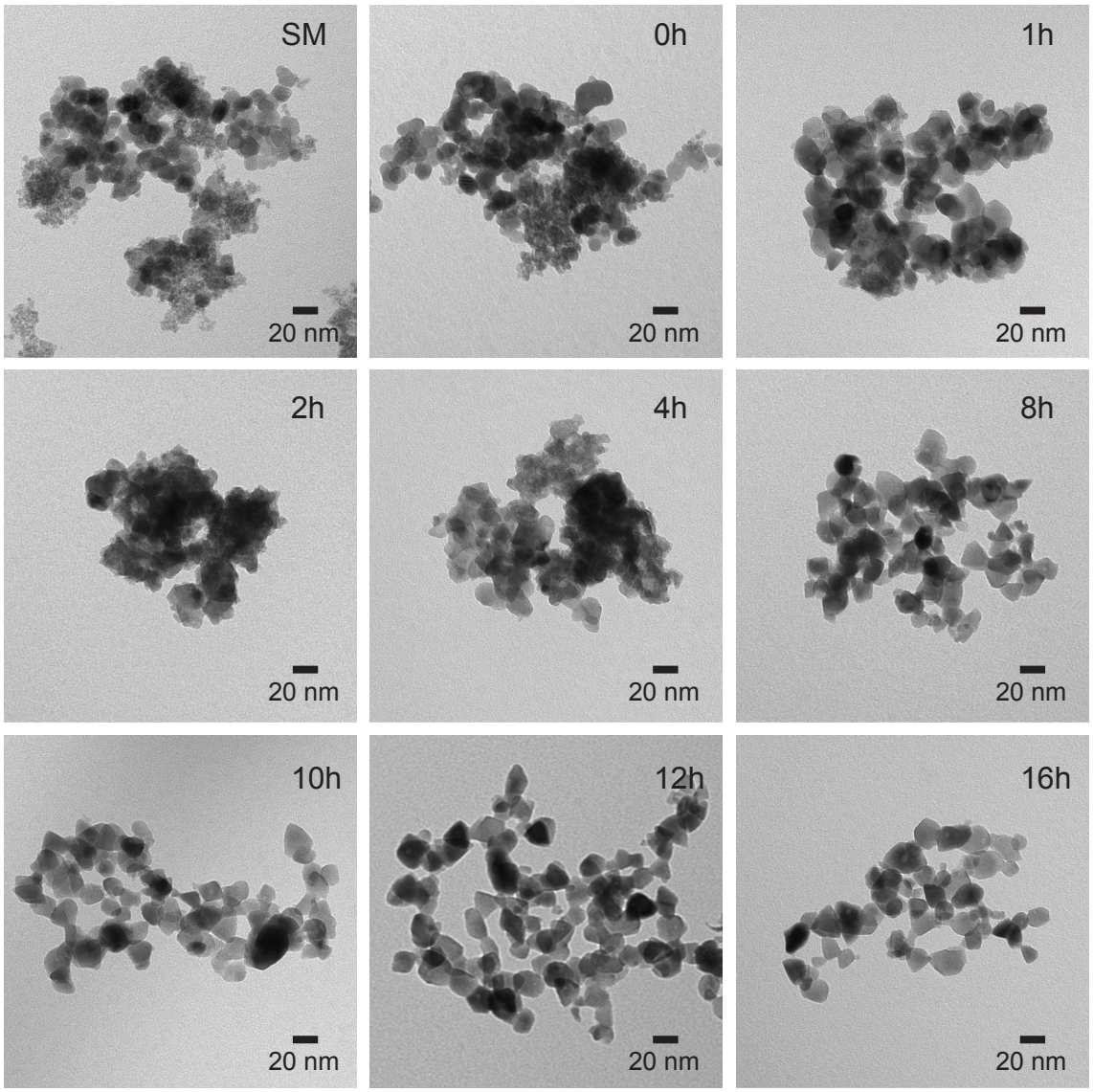

Figure S2. Low-magnification TEM images of the nitrided products for 0–16 hours at 650 ºC from a starting material mixture with Zn/(Zn+Ga)=0.39.

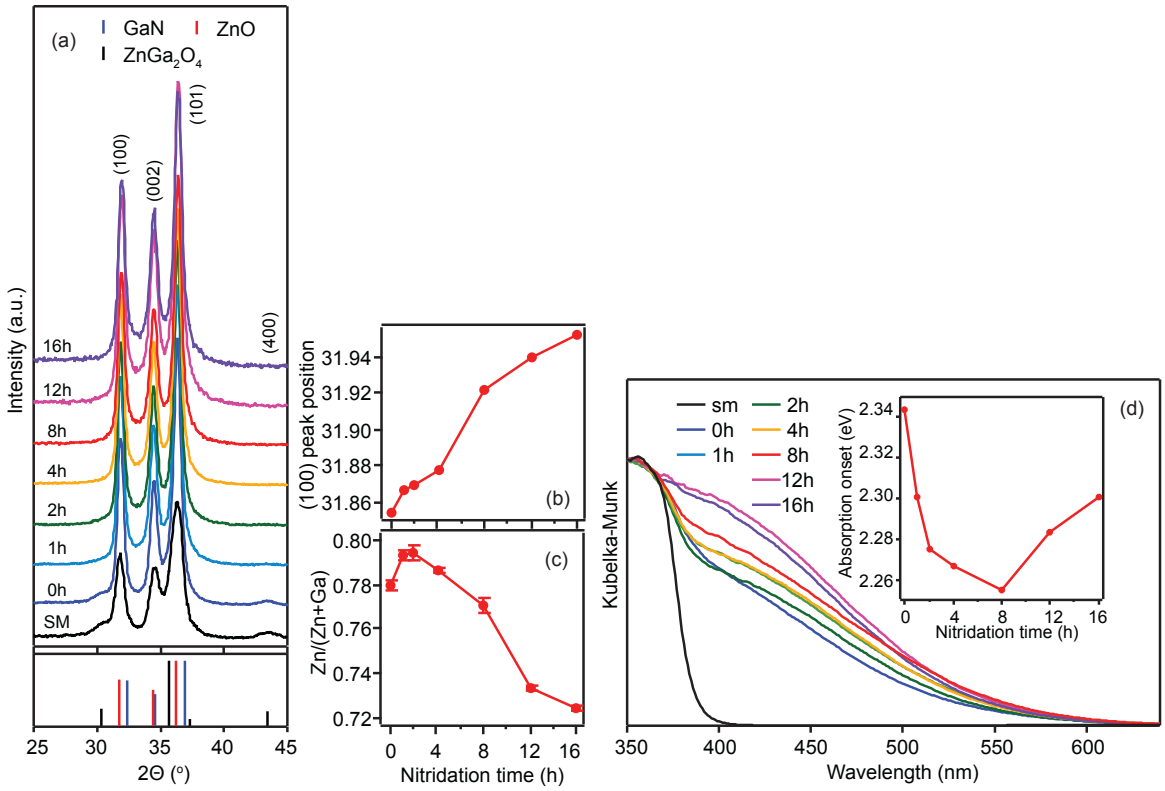

Figure S3. (a) Powder XRD patterns, (b) (100) peak position, (c) Elemental analysis from ICP-OES, and (d) Diffuse reflectance spectra (normalized at 350 nm) of the products from nitridation of a starting mixture (Zn/(Zn+Ga)=0.78).

As shown in Figure S3, ZnO-rich starting mixture (Zn/(Zn+Ga)=0.78) was nitrided for 0 - 16 hours. The XRD patterns of each nitrided product show that the spinel peaks of $ZnGa_2O_4$ in the starting mixture quickly disappear, and the (100) peak of ZnO shifts to higher angle in 2 hours of nitridation, resulting from the conversion of spinel $ZnGa_2O_4$ and wurtzite ZnO to wurtzite $(Ga_{1-x}Zn_x)(N_{1-x}O_x)$, similar to what we observed from the x=0.39 sample set described in the manuscript. The shift of the wurtzite (100) peak was not drastic in this ZnO-rich sample set since the starting mixture contains much smaller amount of $ZnGa_2O_4$ than that in the x=0.39 sample set. Zn loss appeared to be significant (on the order of 10%) after 2 hours of nitridation in the x=0.78 synthesis, which leads to the changes of the (100) peak position observed after 2 hours. The Zn loss is caused by reduction of ZnO to Zn under ammonia atmosphere, and subsequent volatilization of the Zn. This results in the peak shift towards GaN observed after 2 hours. In the diffuse reflectance spectra of the nitrided products, the absorption onsets rapidly shift to lower energy as the spinel $ZnGa_2O_4$ and wurtzite ZnO convert to wurtzite $(Ga_{1-x}Zn_x)(N_{1-x}O_x)$ in the same time period. In conclusion, the observations from both ZnO-low and ZnO-rich sample sets reveal the consistent reaction mechanism where the conversion of spinel $ZnGa_2O_4$ to wurtzite occurs upon topotactic nucleation at a ZnO/ $ZnGa_2O_4$ interface, and this results in the red shift of absorption onsets.

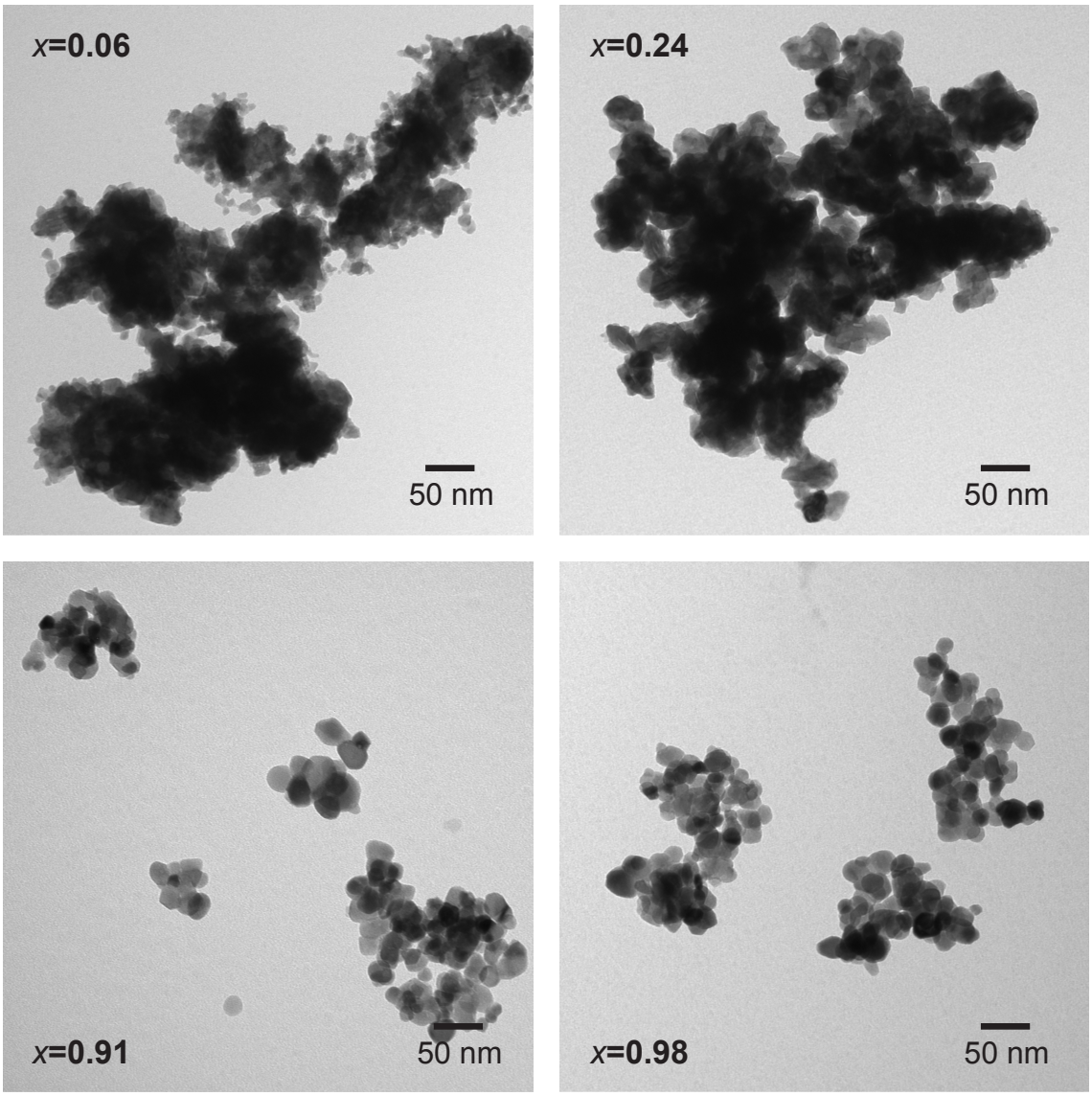

Figure S4. Low magnification TEM images of $(Ga_{1-x}Zn_x)(N_{1-x}O_x)$, ($x$=0.06, 0.24, 0.91, and 0.98).

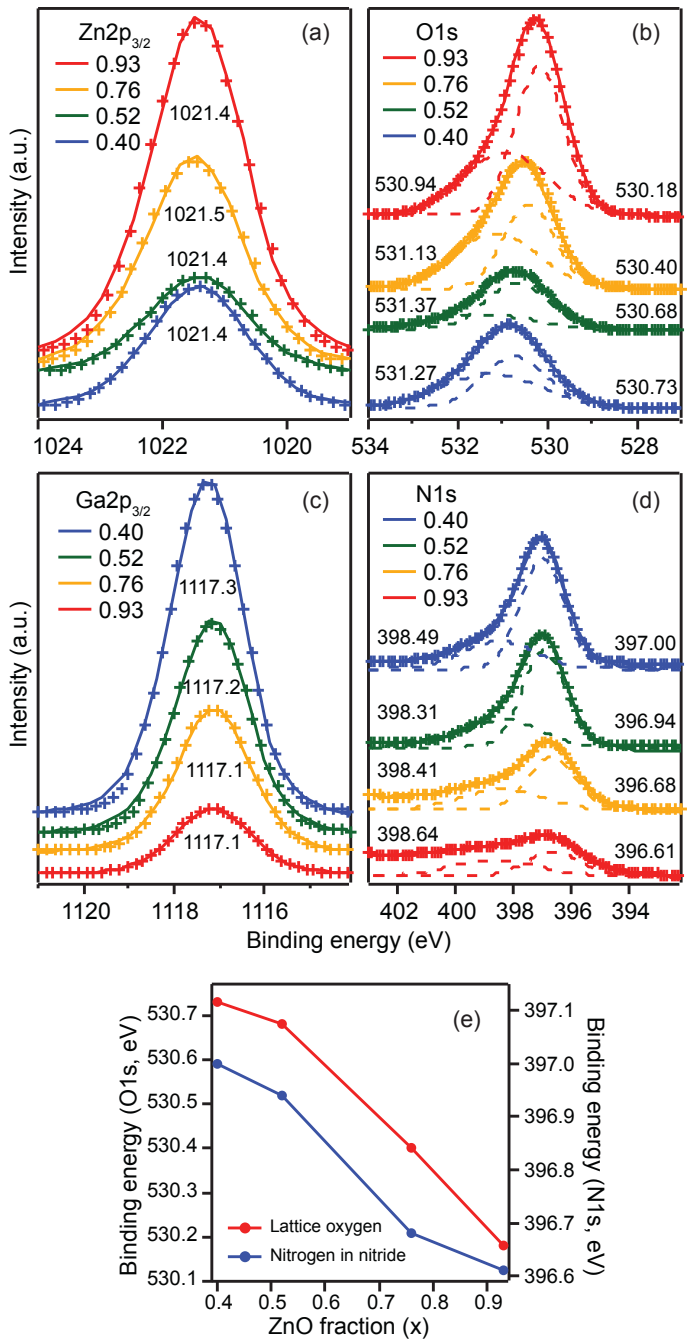

Figure S5. XPS spectra of the $(Ga_{1-x}Zn_x)(N_{1-x}O_x)$ with x= 0.40, 0.52, 0.76, and 0.93 for (a) $Zn2p_{3/2}$, (b) O1s, (c) $Ga2p_{3/2}$, and (d) N1s. (e) Binding energy of lattice oxygen (red) and nitrogen in nitride (N^{3-}) versus the x value.

Figure S5 shows the high-resolution XPS spectra for the O1s and N1s peaks of $(Ga_{1-x}Zn_x)(N_{1-x}O_x)$ with x=0.40, 0.52, 0.76, and 0.93. The $Zn2p_{3/2}$ peaks of the $(Ga_{1-x}Zn_x)(N_{1-x}O_x)$ appear at almost the same binding energy (1021.4–1021.5 eV) regardless of the composition, which is lower than the reference value of ZnO (1022.0 eV[1]) as shown in Figure S5a. This indicates that Zn in $(Ga_{1-x}Zn_x)(N_{1-x}O_x)$ has more electron density than in ZnO. The same behavior was observed in bulk $(Ga_{1-x}Zn_x)(N_{1-x}O_x)$ and was attributed to the presence of Zn-N bonding and

lower electronegativity of N than O.[2] The O1s peaks in Figure S5b were deconvoluted into two peaks that can be assigned to a crystal lattice oxygen (530.18–530.73 eV) and surface –OH group (531.13–531.37 eV).[2] The peaks of the lattice oxygen appear at lower energies with increasing *x*, as shown in Figure S5e. The peak shift with composition suggests the existence of Ga-O bonds as well as Zn-O bonds in the lattice and the amount of each bonding changes with the composition. Higher *x* samples contain less Ga-O bonding and more Zn-O bonding, leading to the movement of more electron density towards O due to lower electronegativity of Zn than Ga (electronegativity: 1.65 for Ga; 1.81 for Zn based on Pauling scale).[3] For $Ga2p_{3/2}$ peaks (Figure S5c), all the samples show similar peak position at 1117.1–1117.3 which are consistent with $Ga2p_{3/2}$ in GaN (1117.1 eV[4]). Because the reference peak of $Ga2p_{3/2}$ in Ga_2O_3 (1117.5–1117.8[5]) is very close to the one in GaN, the possible presence of the Ga-O bonding as well as the Ga-N bonding cannot be excluded. The N1s peak of all the samples consists of two components (Figure S5d).[6-9] The peak of N1s at ~398.5 eV is similar to that of NH_3 and primary amines. The presence of the amine peak could be due to the NH_3 molecules adsorbed on the surface during the nitridation.[8] The other N1s peak appears at the lower binding energy (396.61–397.00 eV). We assign this peak to nitride (N^{3-}) because the lattice nitrogen peaks of GaN and Zn_3N_2 appear at 397 and 395.7 eV, respectively.[1, 2, 4, 6-9] The nitride peaks continuously shift to lower binding energy with increasing *x* values (see Figure S5e). Similar to the case of oxygen, this shift can be also explained by the existence of Zn-N and Ga-N bonds in the lattice and lower electronegativity of Zn than Ga. With increasing Zn content, more electron density moves toward N lowering its binding energy. While XPS analysis of bulk $(Ga_{1-x}Zn_x)(N_{1-x}O_x)$ has been described previously for a narrow range of compositions,[2, 7, 10] composition-dependent XPS peak shifting over a broad range of compositions has not been reported before. The XPS data in Figure S5 is consistent with formation of Ga-O and Zn-N bonds in $(Ga_{1-x}Zn_x)(N_{1-x}O_x)$ nanocrystals, in agreement with XRD data in Figure 4.

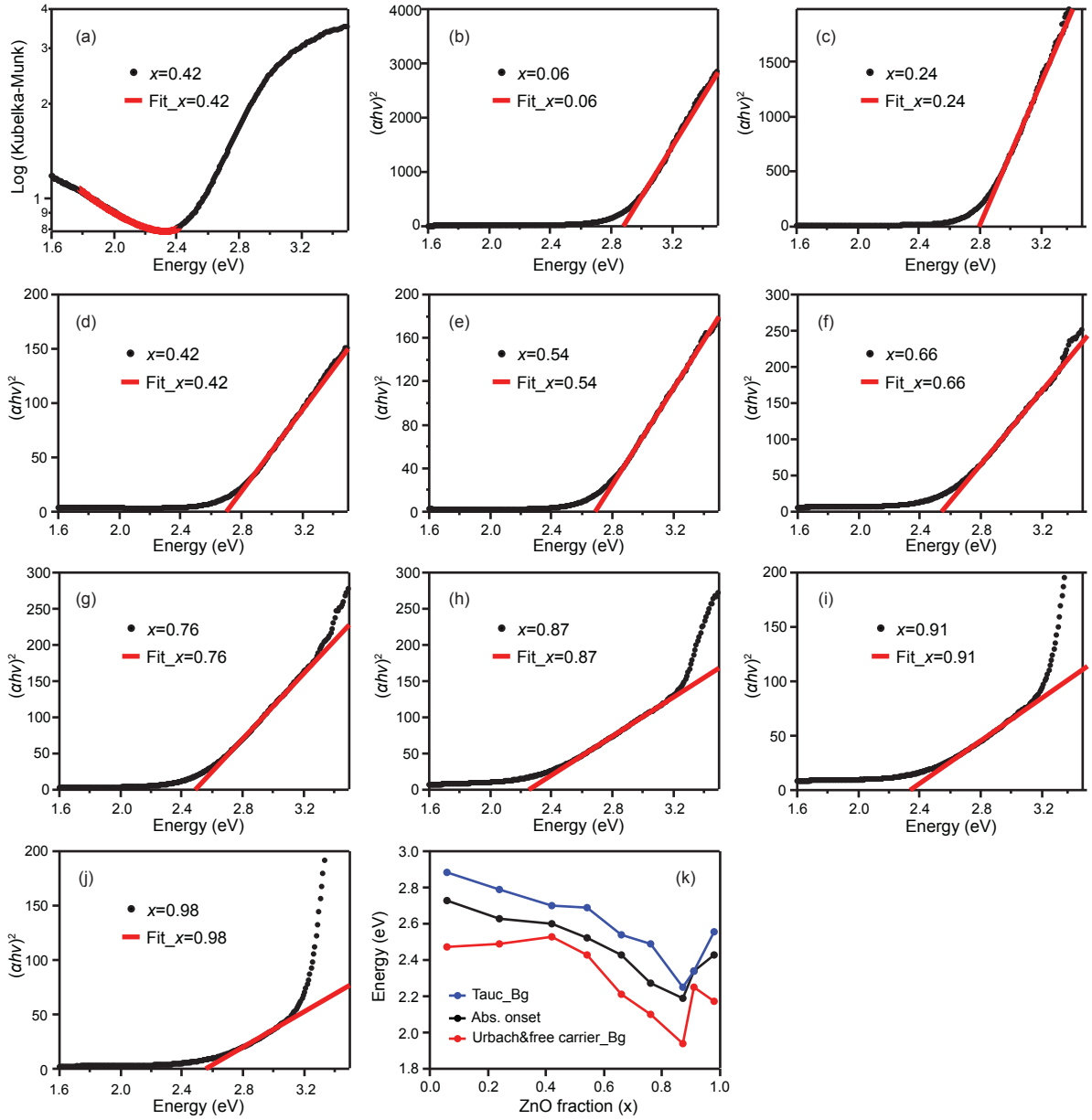

Figure S6. Band gap determination of $(Ga_{1-x}Zn_x)(N_{1-x}O_x)$ from (a) fitting the below-band gap absorption features for x=0.42 sample as previously described.[11] The red line indicates a fit to $\alpha(E) = A \times e^{(E-E_g)/E_u} + B \times E^{-3} + C$, where A, B, and C are constants, E_g is band gap energy, and E_u is Urbach energy. The value of E_g determined by this method is highly dependent on the details of the fit, such as the energy limits. and (b-j) Tauc plots of $(\alpha h\nu)^2$ against $h\nu$. Tauc plot were fit with a straight line (red) below the energy of the absorption feature characteristic of ZnO (3.2 eV). The value of E_g is the x-intercept of the red fit line (k) Band gap energy determined from the direct band gap absorption (Tauc plot), absorption onset, and below-band gap absorption (free carrier + Urbach tail).

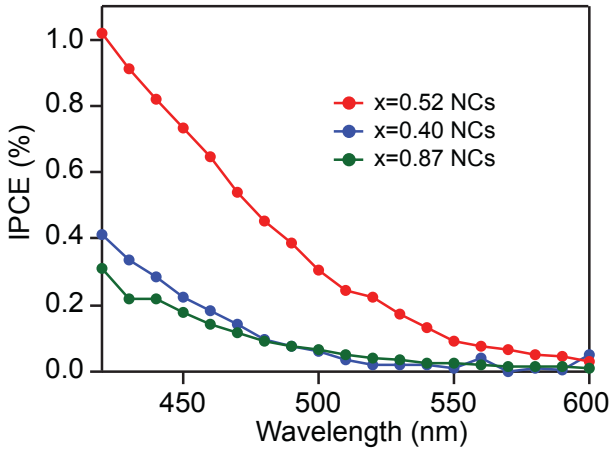

Figure S7. Incident photon-to-current efficiency (IPCE) spectra of nanoscale $(Ga_{1-x}Zn_x)(N_{1-x}O_x)$ (x=0.40, 0.52, and 0.87) obtained from sulfite oxidation in pH 7 phosphate buffer.

References

1. M. Mapa and C. S. Gopinath, *Chem. Mater.*, 2009, **21**, 351-359.
2. K. Maeda, K. Teramura, T. Takata, M. Hara, N. Saito, K. Toda, Y. Inoue, H. Kobayashi and K. Domen, *J. Phys. Chem. B*, 2005, **109**, 20504-20510.
3. G. C. Park, S. M. Hwang, J. H. Choi, Y. H. Kwon, H. K. Cho, S.-W. Kim, J. H. Lim and J. Joo, *Phys. Status Solidi A* 2013, **210**, 1552-1556.
4. N. H. Tran, W. J. Holzschuh, R. N. Lamb, L. J. Lai and Y. W. Yang, *J. Phys. Chem. B*, 2003, **107**, 9256-9260.
5. http://srdata.nist.gov/xps/
6. M. Futsuhara, K. Yoshioka and O. Takai, *Thin Solid Films*, 1998, **317**, 322-325.
7. M. Mapa, K. S. Thushara, B. Saha, P. Chakraborty, C. M. Janet, R. P. Viswanath, C. Madhavan Nair, K. V. G. K. Murty and C. S. Gopinath, *Chem. Mater.*, 2009, **21**, 2973-2979.
8. X. Yang, A. Wolcott, G. Wang, A. Sobo, R. C. Fitzmorris, F. Qian, J. Z. Zhang and Y. Li, *Nano Lett.*, 2009, **9**, 2331-2336.
9. F. Zong, H. Ma, C. Xue, H. Zhuang, X. Zhang, H. Xiao, J. Ma and F. Ji, *Solid State Commun.*, 2004, **132**, 521-525.
10. J. Wang, B. Huang, Z. Wang, P. Wang, H. Cheng, Z. Zheng, X. Qin, X. Zhang, Y. Dai and M.-H. Whangbo, *J. Mater. Chem.*, 2011, **21**, 4562-4567.
11. A. A. Reinert, C. Payne, L. Wang, J. Ciston, Y. Zhu and P. G. Khalifah, *Inorg. Chem.*, 2013, **52**, 8389-8398.